eXtended Discontinuous Galerkin (X-DG) for bi-material elliptic problem

Ahmed Sherif[*], **Michel Visonneau**[*,†], **Ganbo Deng**[*,†], **and Luís Eça**[‡]
[*]ECN, LHEEA, Nantes/France, [†]CNRS, France, [‡]ULisboa/IST, Lisbon/Portugal
ahmed.sherif@ec-nantes.fr

1 Introduction

The development of high-order accurate numerical schemes for Computational Fluid Dynamics (CFD) applications is getting a considerable attention in the research community Wang et al., 2013, Kroll, 2006. When it comes to research in high-order schemes, the family of Discontinuous Galerkin (DG) Finite Element Method (FEM) is very popular.

The flow around a maneuvering ship is a problem of interest in the field of marine engineering. It involves multi-fluid (air-water) flow all within the limit of incompressibility hypothesis. The simulation of such incompressible flow requires an interface-capturing technique to numerically resolve the position of the air-water-ship interfaces when unfitted meshes are employed. An example of such interface-capturing techniques is the Level-Set method. Some work has been done to incorporate the Level-Set method into a DG framework using the concepts of eXtended FEM (X-FEM) Moës et al., 1999, as for instance the work presented in Utz, 2018 leading to the concept of extended DG (X-DG).

In this report, a first step towards the full development of a solver for laminar incompressible multi-fluid flow is shown. A technique to solve a bi-material elliptic problem is introduced. This could represent the step for solving the pressure equation or the Helmholtz equation of the viscous step in a projection method solver for Incompressible Navier-Stokes (INS) equations as in Karniadakis et al., 1991. This first step is composed of implementing the following:

- X-DG solver for *stationary interface* bi-material elliptic problems using linear elements
- X-DG solver for *stationary interface* bi-material elliptic problems using high-order elements
- X-DG solver for *moving interface* bi-material elliptic problems using high-order elements

where only the first point is discussed in this paper.

2 Problem Statement

Let $\Omega \subset \mathbb{R}^d$ be a bounded domain by a boundary $\partial\Omega$. Ω is divided into two disjoint subdomains

$$\overline{\Omega} = \overline{\Omega_1} \cup \overline{\Omega_2}, \qquad \Omega_1 \cap \Omega_2 = \emptyset$$

with an interface

$$\mathcal{I} = \overline{\Omega_1} \cap \overline{\Omega_2}.$$

A bi-material elliptic problem, whose solution presents a weak discontinuity at the interface, is stated as

$$\begin{cases} -\boldsymbol{\nabla}\cdot(\mu\boldsymbol{\nabla}u) = s & \text{in } \overline{\Omega_1} \cup \overline{\Omega_2}, \\ u = u_D & \text{on } \Gamma_D, \\ -\mu\boldsymbol{\nabla}u \cdot \boldsymbol{n} = g_N & \text{on } \Gamma_N, \\ [\![u\boldsymbol{n}]\!] = \boldsymbol{0} & \text{on } \mathcal{I}, \\ [\![\mu\boldsymbol{\nabla}u \cdot \boldsymbol{n}]\!] = 0 & \text{on } \mathcal{I}. \end{cases} \tag{1}$$

where u is the solution to the problem, μ is a material property that is discontinuous across the interface $\mathcal{I}$ (that is, $\mu = \mu_i$ in Ω_i for $i = 1, 2$), s is a known source term, u_D is a prescribed value of the solution on the Dirchlet boundary Γ_D, and g_N is a prescribed normal flux on the Neumann boundary Γ_N, with $\Gamma_D \cup \Gamma_N = \partial\Omega$. The *jump* operator $[\![\odot]\!]$ is defined as:

$$[\![\odot]\!] := \odot_{left} + \odot_{right}.$$

3 Concepts of eXtended Finite Element Method (X-FEM)

3.1 Enrichment Functions in Cut Elements

In the context of X-FEM Moës et al., 1999, Pommier et al., 2011, in an element K_i cut by an interface $\mathcal{I}$, the standard FE polynomial approximation of the solution is enriched by adding extra terms to the interpolation as follows:

$$u|_{K_i}(\boldsymbol{x}) \approx u^h|_{K_i}(\boldsymbol{x}) = \underbrace{\sum_{j=1}^{\mathtt{n_{en}}} N_j(\boldsymbol{x}) u_j}_{\text{Standard FE}} + \underbrace{\sum_{j=1}^{\mathtt{n_{en}}} H(\boldsymbol{x}) N_j(\boldsymbol{x}) a_j}_{\text{Enrichment}} \quad \in \mathcal{V}^h, \quad \text{if } K_i \cap \mathcal{I} \neq \emptyset.$$

where u_j is the value of the solution u at node j, N_j is the polynomial shape function of order k associated to node j, and $\mathtt{n_{en}}$ is the number of nodes per element. In a cut element, the approximation of the solution is enriched by an enrichment function H that allows for the representation of discontinuities within the element, and a_j are the enrichment nodal coefficients. The type and nature of the enrichment function depends on the type of discontinuity to be modelled Sala Lardies et al., 2012.

3.2 Level-Set Representation

The material interface is represented using Level-Set. Basically, a distance function $\phi(\boldsymbol{x})$ is defined that gives the shortest distance between a point and the interface. Assuming that the interface location is known, then each node i of the mesh is assigned a value ϕ_i that provides the information of how far this node is from the interface. The value of ϕ is zero on the interface, negative on one side, and positive on the other side. Furthermore, this distance function is interpolated within an element K_i using the standard FE shape functions as follows

$$\phi|_{K_i}(\boldsymbol{x}) \approx \phi^h|_{K_i}(\boldsymbol{x}) = \sum_{j=1}^{\mathtt{n_{en}}} N_j(\boldsymbol{x}) \phi_j \tag{2}$$

meaning that the Level-Set function is continuous across the interface.

3.3 Modified Intergration in Cut Elements

One of the main ingredients in X-FEM is the modified integration quadrature in each cut element. For this purpose, it is a must to accurately represent the interface within each cut element. A material interface is generally curved. High-order accurate representation of the interface is crucial for optimal convergence, see Cheng and Fries, 2010, Sala Lardies et al., 2012. However, in this paper, only linear approximation of the interface is adopted as a starting point in the development. Furthermore, only the simple case of an interface cutting through an element is discussed, where an interface cuts an element twice at two different edges, this is referred to as *basic* cut. Dealing with more complex cuts is discussed for instance in Gürkan et al., 2017. Fig. 1 summarizes the process for modifying the integration quadrature within the element and on the edges as well.

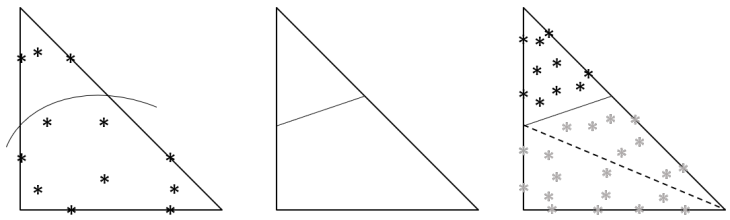

Fig. 1: Element with standard integration points and a curved interface cutting through (left), linear representation of the interface (center), and element with modified quadrature (right). In the right plot, integration points in black are in domain Ω_1 while grey points are in domain Ω_2, which is divided in two sub-domains.

4 Weak Form with no Condition on the Material Interface

The weak form of the bi-material elliptic problem is derived using the concepts discussed in Arnold et al., 2000, Arnold et al., 2002, Hartmann, 2008, where the mixed strong form of the problem is considered and Symmetric Interior Penalty (SIP) approximation for the DG numerical fluxes are employed, see Hesthaven and Warburton, 2007 for further details.

Using the *ridge enrichment* function presented in Moës et al., 2003 which is defined as:

$$H(\boldsymbol{x}) = \sum_i N_i(\boldsymbol{x})|\phi_i| - |\sum_i N_i(\boldsymbol{x})\phi_i| \tag{3}$$

and plotted for a 1D linear element as shown in Fig. 2, results in the following weak form:

$$\begin{aligned}(\boldsymbol{\nabla} v, \mu \boldsymbol{\nabla} u^-)_{K_i} &- \frac{1}{2}\langle \boldsymbol{\nabla} v, \mu(u^- - u^+)\boldsymbol{n}^-\rangle_{\partial K_i \setminus \partial\Omega} - \frac{1}{2}\langle v, \mu(\boldsymbol{\nabla} u^- + \boldsymbol{\nabla} u^+)\cdot \boldsymbol{n}^-\rangle_{\partial K_i \setminus \partial\Omega} \\ &+ \langle v, \mu\tau(u^- - u^+)\rangle_{\partial K_i \setminus \partial\Omega} \\ &- \langle \boldsymbol{\nabla} v, \mu u^- \boldsymbol{n}^-\rangle_{\partial K_i \cap \Gamma_D} - \langle v, \mu \boldsymbol{\nabla} u^- \cdot \boldsymbol{n}^-\rangle_{\partial K_i \cap \Gamma_D} + \langle v, \mu\tau u^-\rangle_{\partial K_i \cap \Gamma_D} \\ &= (v, s)_{K_i} - \langle v, g_N\rangle_{\partial K_i \cap \Gamma_N} - \langle \boldsymbol{\nabla} v, \mu u_D \boldsymbol{n}^-\rangle_{\partial K_i \cap \Gamma_D} + \langle v, \mu\tau u_D\rangle_{\partial K_i \cap \Gamma_D}\end{aligned} \tag{4}$$

where the variables with superscript $^-$ belong to the element K_i while that with superscript $^+$ belong to the adjacent element.

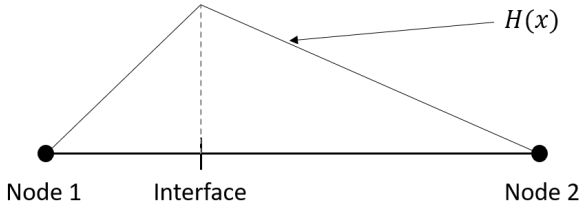

Fig. 2: The *ridge enrichment* function given by Eq. (3) in a 1D linear element.

5 Numerical Example

The bi-material heat problem introduced in Sec. 2 is solved in this section using the eXtended Discontinuous Galerkin (X-DG) method. A problem with known exact solution is presented in Gürkan et al., 2017. In this example a circular interface $\mathcal{I}$ with radius $R = 0.5$ is considered to divide the square domain $\Omega = [-1, 1]^2$ into two to regions, Ω_1 and Ω_2, as shown in Fig. 3. The heat distribution over a plate, which is made of two materials with different thermal conductivities, is computed. The thermal conductivities and the analytical solution are defined by:

$$\mu(\boldsymbol{x}) = \begin{cases}\mu_1 = 100 & \text{in } \Omega_1 \\ \mu_2 = 1 & \text{in } \Omega_2\end{cases} \qquad u(\boldsymbol{x}) = \begin{cases}\dfrac{1}{\mu_1}(x^2 + y^2)^{5/2} & \text{in } \Omega_1 \\ \dfrac{1}{\mu_2}(x^2 + y^2)^{5/2} + \left(\dfrac{1}{\mu_1} - \dfrac{1}{\mu_2}\right)R^5 & \text{in } \Omega_2\end{cases}$$

The corresponding source term is $s = -25(x^2 + y^2)^{3/2}$, Dirichlet boundary conditions are set on the boundary. The problem is solved using the X-DG method with linear ($p = 1$) triangular elements. Six meshes are used where the initial mesh is isotropically refined in each refinement. The respective recorded errors in the $\mathcal{L}_2$-norm are shown in Table 1, and the mesh convergence plot is shown in Fig. 4. It is noticed that optimal convergence of order ($p + 1$, i.e. 2) is not achieved, in fact, the plot shows non-monotonic convergence.

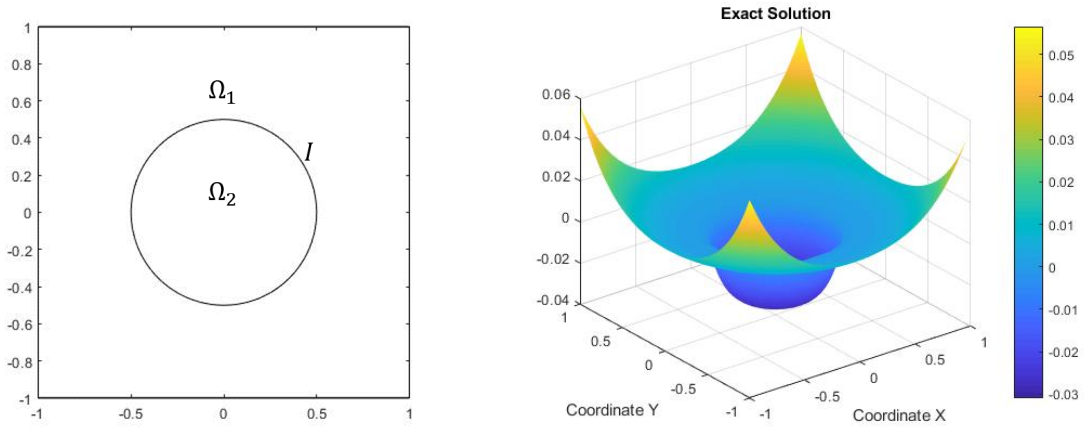

Fig. 3: Square domain with circular interface (left), analytical solution (right).

$\mu_1 = 100, \mu_2 = 1$ - X-DG solver						
Mesh	error $\mathcal{L}_2$-norm	size of the discrete operator	% of cut elements with area ratio > 9	maximum area ratio in cut elements	condition number of the discrete operator	maximum absolute residual $\boldsymbol{AU}_{enr}$-$\boldsymbol{f}$
mesh 1	3.9866	720^2	40%	17 : 1	1.1408e+11	3.4e−13
mesh 2	0.0480	$2,568^2$	29%	108 : 1	4.3237e+08	1.7e−13
mesh 3	0.0142	$10,008^2$	41%	419 : 1	6.1022e+10	1.7e−13
mesh 4	0.0969	$39,288^2$	43%	1,639 : 1	3.2652e+11	2.2e−13
mesh 5	0.0165	$155,496^2$	45%	6,479 : 1	2.3599e+11	2.8e−13
mesh 6	0.0096	$618,216^2$	43%	3,062 : 1	2.2869e+15	2.9e−13

Table 1: Data from the convergence study of the X-DG solver for the bi-material problem with $\mu_1 = 100$ and $\mu_2 = 1$.

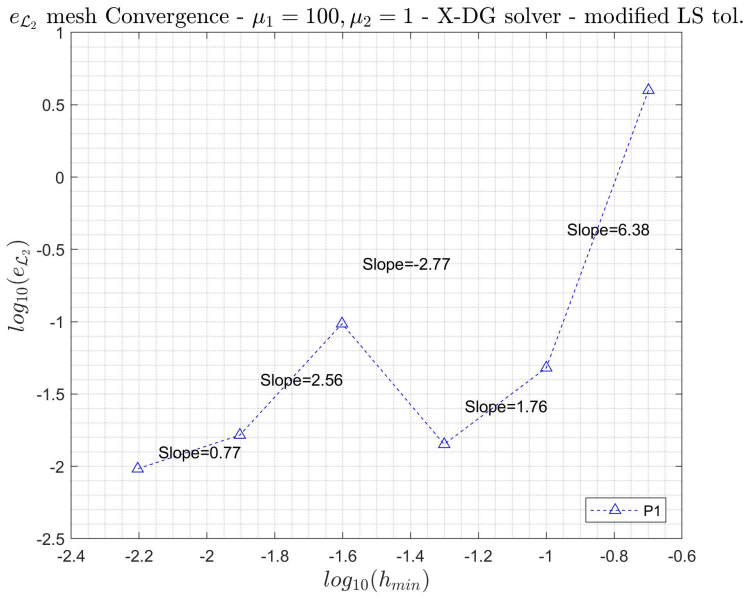

Fig. 4: Convergence plot of the X-DG solver for the bi-material problem with $\mu_1 = 100$ and $\mu_2 = 1$.

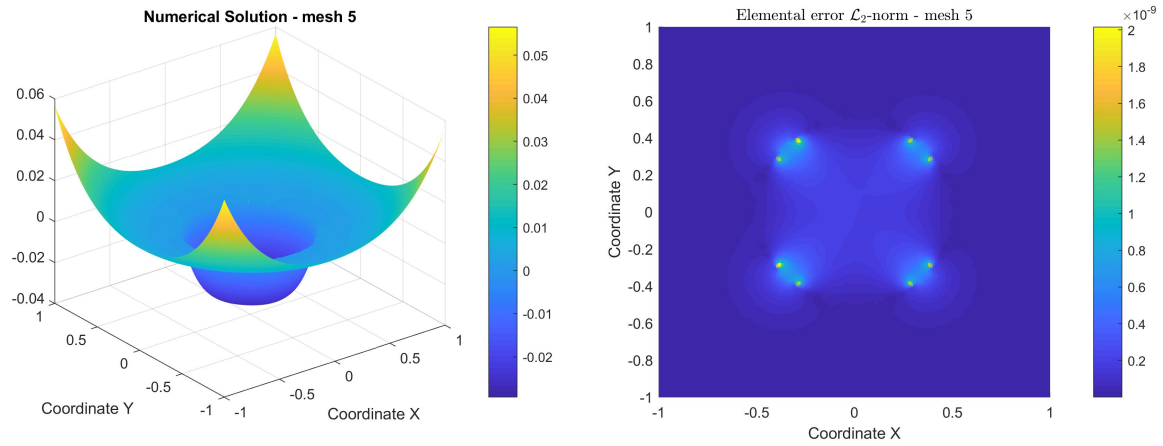

Fig. 5: The numerical solution (left) and the elemental errors $\mathcal{L}_2$-norm (right) for mesh 5.

However, by checking the solution itself and the local elemental errors in $\mathcal{L}_2$-norm, for instance in mesh 5, in Fig. 5, it is noticed that the overall error is dominated by the local errors of some cut elements which are divided by the interface into two regions; one region is very small compared to the other.

To better represent the quality of the cut, we introduce an elemental area ratio, defined as $max(A_1/A_2, A_2/A_1)$; where A_i is the area of the region in domain Ω_i within each cut element. Note that the area ratio is only defined in the cut elements.

A bad-cut is defined as a cut that gives an area ratio greater than 9 Gürkan et al., 2017. For each mesh, the percentage of cut elements with bad-cut situations is recorded in Table 1. These bad-cuts lead to an ill-conditioned discrete operator with very large condition number as recorded in Table 1.

In the literature, for instance in Gürkan et al., 2017, the authors showed optimal convergence using the eXtended Hybridizable DG (X-HDG) for the same problem but they modify the mesh whenever a situation of bad-cut arises. However, as they also reported, this is not a solution, it is just a temporary modification to show that the X-HDG method can converge optimally. To solve this issue of ill-conditioning, further stabilization strategies are used, for instance the strategy based on Nitsche's method Hansbo and Hansbo, 2002. This is going to be the near future work.

6 Conclusions and Near-Future Work

Preliminary results for the bi-material Poisson's problem using X-DG method were shown. The problem was steady, i.e. with stationary material interface. Linear elements were used and the solution was enriched using *ridge enrichment* in the cut elements, i.e. the weak formulation had no interface integrals. The results obtained in the initial tests showed convergence issues because of the situations of bad-cut where the interface divides an element into two regions, one is very small compared to the other.

The near-future work will be:

- Solve the convergence issues resulting from bad-cuts.
- Extend the X-DG solver to accommodate high-order approximation of the solution and the interface, and according to the literature Sala Lardies et al., 2012, this would require the use of *Heaviside enrichment* to recover the optimal convergence.
- Move to problems with moving interface where the interface is described explicitly.
- Move to problems with moving interface where the interface is described implicitly using the Level-Set method.
- Start the implementation for laminar incompressible multi-fluid flow problems.

Acknowledgements

This project is part of Marie Sklodowska-Curie ITN-EJD ProTechTion funded by the European Union Horizon 2020 research and innovation program with grant no. 764636.

References

Arnold, D. N., Brezzi, F., Cockburn, B., and Marini, D. (2000). Discontinuous Galerkin methods for elliptic problems. In *Discontinuous Galerkin Methods*, pages 89–101. Springer.

Arnold, D. N., Brezzi, F., Cockburn, B., and Marini, L. D. (2002). Unified analysis of discontinuous Galerkin methods for elliptic problems. *SIAM journal on numerical analysis*, 39(5):1749–1779.

Cheng, K. W. and Fries, T.-P. (2010). Higher-order XFEM for curved strong and weak discontinuities. *International Journal for Numerical Methods in Engineering*, 82(5):564–590.

Gürkan, C., Kronbichler, M., and Fernández-Méndez, S. (2017). eXtended hybridizable discontinuous Galerkin with Heaviside enrichment for heat bimaterial problems. *Journal of scientific computing*, 72(2):542–567.

Hansbo, A. and Hansbo, P. (2002). An unfitted finite element method, based on Nitsche method, for elliptic interface problems. *Computer methods in applied mechanics and engineering*, 191(47-48):5537–5552.

Hartmann, R. (2008). Numerical analysis of higher order discontinuous Galerkin finite element methods.

Hesthaven, J. S. and Warburton, T. (2007). *Nodal discontinuous Galerkin methods: algorithms, analysis, and applications*. Springer Science & Business Media.

Karniadakis, G. E., Israeli, M., and Orszag, S. A. (1991). High-order splitting methods for the incompressible Navier-Stokes equations. *Journal of computational physics*, 97(2):414–443.

Kroll, N. (2006). ADIGMA: A European project on the development of adaptive higher order variational methods for aerospace applications. In *47th AIAA Aerospace Sciences Meeting including The New Horizons Forum and Aerospace Exposition*, page 176.

Moës, N., Cloirec, M., Cartraud, P., and Remacle, J.-F. (2003). A computational approach to handle complex microstructure geometries. *Computer methods in applied mechanics and engineering*, 192(28-30):3163–3177.

Moës, N., Dolbow, J., and Belytschko, T. (1999). A finite element method for crack growth without remeshing. *International journal for numerical methods in engineering*, 46(1):131–150.

Pommier, S., Gravouil, A., Combescure, A., and Moës, N. (2011). *Extended finite element method for crack propagation*. Wiley Online Library.

Sala Lardies, E., Fernández Méndez, S., and Huerta, A. (2012). Optimally convergent high-order X-FEM for problems with voids and inclusions. In *ECCOMAS 2012: 6th European Congress on Computational Methods in Applied Sciences and Engineering. Programme book of abstracts, September 10-14, 2012, Vienna, Austria*, pages 1–14.

Utz, T. (2018). *Level set methods for high-order unfitted discontinuous Galerkin schemes*. PhD thesis, Technische Universität.

Wang, Z. J., Fidkowski, K., Abgrall, R., Bassi, F., Caraeni, D., Cary, A., Deconinck, H., Hartmann, R., Hillewaert, K., Huynh, H. T., et al. (2013). High-order CFD methods: current status and perspective. *International Journal for Numerical Methods in Fluids*, 72(8):811–845.